Eur. Phys. J. D **4**, 181–187 (1998)

THE EUROPEAN PHYSICAL JOURNAL D

Molecular spectra, quantum chaos, and scars

F.J. Arranz[1], F. Borondo[1,a], and R.M. Benito[2]

[1] Departamento de Química, C–IX, Universidad Autónoma de Madrid, Cantoblanco, 28049 Madrid, Spain
[2] Departamento de Física y Mecánica, Escuela Técnica Superior de Ingenieros Agrónomos, Universidad Politécnica de Madrid, 28040 Madrid, Spain

Received: 16 March 1998 / Revised: 23 April 1998 / Accepted: 4 May 1998

Abstract. Low resolution features in the spectra of classically chaotic atomic and molecular systems are known to be related to recurrences induced by classical periodic motions. In this paper we study how such characteristics reveal in the LiNC/LiCN isomerizing molecular system, and describe how the transition from regularity to classical chaos that takes place in this system shows up at quantum level in the structure of the corresponding wavefunctions in the form of "scars". To this end we use some projection techniques, based on the propagation of wave packets, which have been developed in our laboratory. In this way some regions at the border of the chaotic region can be detected, in which the systematics of "scar" formation can be studied at a very elementary level, without complications due to the high level density which are customarily used in this type of studies in order to achieve the semiclassical limit.

PACS. 05.45.+b Theory and models of chaotic systems – 03.65.Sq Semiclassical theories and applications

1 Introduction

Modern spectroscopic techniques provides a wealth of information about atoms and molecules, from data concerning their structural characteristics to valuable insight about related dynamical processes, such as photodissociation, isomerization reactions, intramolecular energy transfer, *etc.* [1].

Typical studies in traditional vibrational spectroscopy were usually concerned only with low lying vibrational states, in which the nuclei move in a region localized around the minimum of the Born-Oppenheimer potential energy surface. Perturbations were also considered in the form of (weak) anharmonicities, being responsible for overtone and combination frequencies [2]. In this regime, the intramolecular dynamics are completely regular. Spectra consist, at least in the ideal case, of a progression of bands, corresponding to the different excitations in each normal mode, being in principle easily assignable, due to the lack of irregularities.

This simplicity is a reflection of the fact that the corresponding wave functions exhibit a very regular nodal pattern [3], where the corresponding quantum numbers can also be assigned easily (by visual inspection, for example). Nonetheless, special attention should be paid to the case where classical resonances are present. When these classical features are important [4,5], they have a profound influence on the nodal structure of wave functions, as demonstrated by Heller *et al.* [6].

At higher levels of excitation the dynamics of molecular systems change drastically, and the interactions between normal modes [4,5] make the structure of the spectra to become more complicated. From a classical point of view, this behaviour is well-understood in terms of the KAM (Kolmogorov-Arnold-Moser) theorem [7], which dictates that, as the perturbation induced by increasing the energy grows, thus deviating from the quadratic regime, more regular tori are destroyed, rendering a multitude of resonant chains of islands, overlapping bands of stochasticity, and embedded cantori acting as dynamical bottlenecks [8]. Non-linear interactions among normal modes lead to irreversible intramolecular vibrational energy flow, which is controlled by all classical structures mentioned above. Also, the rate of many intramolecular dynamical processes: unimolecular decomposition, isomerization, *etc.*, is determined by this intramolecular vibrational relaxation (IVR) [9].

Recently, the traditional approach has changed importantly by the introduction of many new spectroscopic techniques, such as IR overtone excitation, multiphoton excitation, stimulated emission pumping (SEP) or electron photodetachment [10,11], in which extensive regions of the potential energy surface, sometimes very far from the equilibrium geometries, are probed.

On the theoretical side, efficient methods have been developed in the near past for the accurate calculation of eigenvalues and eigenfunctions of the vibrationally very excited states necessary to interpret these new spectra, and also to carry out time-dependent quantum dynamical studies [12,13]. Among the first, those based on the

[a] e-mail: f.borondo@uam.es

discrete variable representation (DVR) method [14] deserve special mention for their outstanding performance.

In this high energy regime, the interpretation of the corresponding wave functions in simple terms is much more difficult. For moderate excitation energies, choosing adequate (curvilinear) coordinate system [15] can help. But on the other hand, for very high vibrational energies some wave functions appear localized on classical periodic orbits (PO) of the system [16]. Periodic orbits are classical trajectories which retrace themselves. In the case that they correspond to a stable motion, that is, when small deviations in the initial conditions result in altered motion which remains close to the initial orbit, the localization has been explained as the result of a focalization effect [12].

More difficult to understand, still remaining an unsolved question in the field of quantum chaos [17], is the localization by unstable POs, since the dynamics in their vicinity is such that neighbour trajectories diverge exponentially [18]. This localization effect, known also as "scarring", was first discussed by Heller [19] in his numerical study of very highly excited states of the stadium billiard [20], a system that exhibits all properties in the hierarchy of chaos. This observation came as a surprise, since for the high lying states of classically chaotic systems, a more uniform distribution of the quantum density was expected [21], according to the results of Shnirelman theorem [22].

The pioneering work of Gutzwiller [23] some years before had demonstrated the importance of POs in the quantization of classically chaotic systems. Unstable POs constitute the only remnants of order in systems exhibiting hard chaos. Some important advances have been made since them. For example, Bogomolny [24] demonstrated, using Gutzwiller's summation formulas, that the quantum probability density smoothed over small ranges in energy and space has, superimposed to the microcanonical distribution term, contributions localized around closed classical paths. This implies that scars are not *in general* a property of single eigenfunctions, but should generically be associated with groups of eigenstates, defined by the aforementioned energy range. Actually, it was shown by our group [25] how the right combination of eigenfunctions that is scarred by a particular PO can be constructed. Moreover, we also studied [26] the systematics of scar formation at its most elementary level by considering correlation diagrams taking $\hbar$ as a parameter. In this way, the frontier between chaos and order could be attained, and showed how only two interacting states are needed to form a scar. The chaotic character of a quantum state can be assesed by examination of the distribution of zeros [27] of the corresponding Husimi function [28]. This property, which has not received as much attention in the literature as the corresponding maxima, constitutes a very sensitive criterion: in the case of regular states the zeros of the Husimi function all lie on a line; while for more stochastic ones the zeros appear uniformly distributed over the whole available phase space. Scarred states can also be detected with this method [29].

Periodic orbits can also be used to numerically compute spectra [30,31]. When the dynamics are very complex it can only be fully resolved if long time propagations are considered [32]; conversely if only low resolution is required merely the details of short trajectories or pieces of trajectories are needed [33,34].

In this paper we discuss some implications of the order-chaos transition in molecular spectra, specially in relation to how this is reflected in the structure of the corresponding wave functions as energy increases. For this purpose we will make use of some novel techniques, based in the propagation of wave packets that have been developed in our laboratory.

The organization of the paper is as follows. In Section 2 we describe the model for the LiCN molecule used in our study, and the different type of calculations reported. In Section 3 some results corresponding to the simulation of SEP-type spectra are presented and analyzed using classical and quantal arguments. Finally, in Section 4 we conclude by summarizing our conclusions and remarks.

2 Model and calculations

As our working example, we choose the vibrational dynamics of a triatomic molecule: the LiNC/LiCN isomerizing system, which has been extensively studied in the literature [35]. This molecule presents two stable isomers, corresponding to the linear configurations, Li–NC and Li–CN, which are separated by a relatively modest energy barrier of 3454 cm^{-1}. The motion in the bending coordinate is very floppy, and then the Li atom can easily rotate around the CN fragment. Thus, chaos sets in at low values of the excitation energy. Also, the C–N vibrational frequency is very high and separates from the remaining modes of the system.

Accordingly, the dynamics of the system can be adequately studied by a two degrees of freedom model, where the CN distance is kept frozen at its equilibrium value of $r_e = 2.186$ a.u. The vibrational (total $J = 0$) Hamiltonian in scattering or Jacobi coordinates is given by

$$H = \frac{P_R^2}{2\mu_1} + \frac{1}{2}\left(\frac{1}{\mu_1 R^2} + \frac{1}{\mu_2 r^2}\right) P_\theta^2 + V(R,\theta), \qquad (1)$$

where R is the distance between the Li atom and the centre of mass of the CN fragment, r the C–N distance, θ the angle formed by these two vectors, and $\mu_1^{-1} = m_{\text{Li}}^{-1} + (m_{\text{C}} + m_{\text{N}})^{-1}$ and $\mu_2^{-1} = m_{\text{C}}^{-1} + m_{\text{N}}^{-1}$ the Li–CN and C–N reduced masses respectively.

The potential energy surface is a nine terms expansion in Legendre polynomials

$$V(R,\theta) = \sum_{\lambda=0}^{9} P_\lambda(\cos\theta) v_\lambda(R) \qquad (2)$$

where the coefficients v_λ contain short and long-range contributions, and have been taken from the literature [36]. Very recently, a new *ab initio* surface has been reported

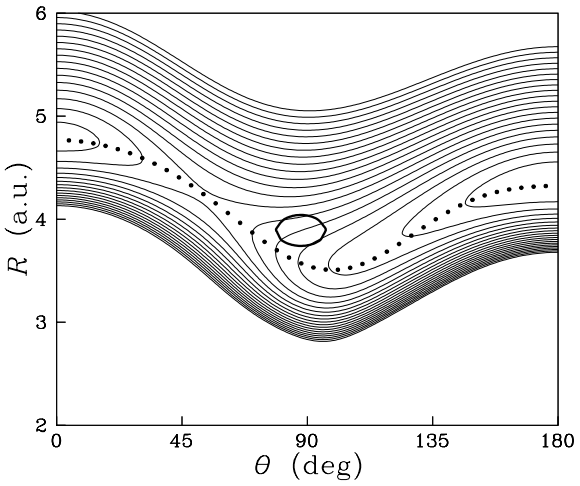

Fig. 1. Contour plot of the potential energy surface for the LiNC/LiCN isomerizing system. The minimum energy path connecting the two stable linear isomers (Li–NC at $\theta = 180°$ and Li–CN at $0°$), and the initial Gaussian wave packet used to generate the spectrum of Figure 2 are also shown.

[37] that includes electron correlation at MP4 level. The differences between them are small, except for the existence in the new one of a stable T-shaped minimum in the region around $(R, \theta) = (3.65 \text{ a.u.}, 110°)$, where the surface of Essers *et al.* only shows a plateau. However, this difference is dynamically not very significant since the motion around this plateau gets stabilized by an adiabatic separation mechanism for high value of the excitation in the R coordinate, as has been demonstrated by us [38]. In Figure 1 a contour plot of the Essers *et al.* energy surface is presented. The two stable isomers LiNC and LiCN, appearing respectively at $(R, \theta) = (4.3487 \text{ a.u.}, 180°)$ and $(4.7947 \text{ a.u.}, 0°)$ are clearly visible as potential wells separated 2281 cm^{-1}. The minimum energy path, $R_e(\theta)$, connecting these two wells is also been plotted as a dotted line.

Classical trajectories have been calculated using a fixed step Gear algorithm for the numerical integration of Hamilton equations of motion corresponding to equation (1). The isomerization process can be followed by considering the motion along the θ coordinate. This is most significantly done by means of Poincaré surfaces of section (SOS) in phase space. Usually, SOS for systems of coupled oscillators are obtained by plotting one coordinate and its conjugate momentum every time that the other coordinate crosses through its equilibrium distance, and the momentum has a predetermined sign. In our case, this corresponds to crossing the minimum energy path, $R_e(\theta)$, and this causes a new problem to rise since R_e varies with θ. Thus, in order to make the SOS an area preserving map, the following set of canonical coordinates

$$\begin{aligned} &\rho = R - R_e(\theta), \qquad \psi = \theta, \\ &P_\rho = P_R, \qquad\qquad P_\psi = P_\theta + P_R \left(\frac{\partial R_e}{\partial \theta}\right)_{\theta=\psi}, \end{aligned} \tag{3}$$

have been used [39]. The SOS corresponds then to the successive intersections of each trajectory with the $\rho = 0$ plane, taking only those points for which P_ρ is in a predetermined branch of the second degree equation

$$H(\rho = 0, \psi, P_\rho, P_\psi) = E. \tag{4}$$

The quantum vibrational energy levels and corresponding wave functions for the LiNC/LiCN system were calculated using the program of Bačić and Light [40], which uses a DVR representation in the θ coordinate and a distributed Gaussian basis (DGB) in the radial coordinate R. A prediagonalization along each θ ray prepares the final basis set, that with 2016 elements rendered the 900 low lying eigenvalues converged to within 0.1 cm^{-1}.

A very convenient way to compare the quantum results with classical trajectory calculations is to consider wave packets evolution. The center of these non-stationary functions follows during a certain time close to classical paths, without excessive spreading of the packet. In our case the dynamics of such wave packets can be calculated quite easily by projection of the initial function into the basis set formed by the stationary eigenstates of the system, $|n\rangle$, followed by the application of the corresponding evolution operator

$$|\Phi(t)\rangle = e^{-i\hat{H}t/\hbar}|\Phi(0)\rangle = \sum_n |n\rangle\langle n|\Phi(0)\rangle \; e^{-iE_n t/\hbar}. \tag{5}$$

This evolution can be followed either in the time domain by the recurrences of the corresponding correlation function:

$$C(t) = \langle\Phi(0)|\Phi(t)\rangle, \tag{6}$$

or in the energy domain with the corresponding spectrum:

$$I(E) = \sum_n |\langle n|\Phi(0)\rangle|^2 \; \delta(E - E_n). \tag{7}$$

These two quantities are related by Fourier transform [32],

$$\begin{aligned} I(E) &= \textstyle\sum_n \; |\langle n|\phi(0)\rangle|^2 \; \delta(E - E_n) \\ &= \; (1/2\pi\hbar) \; \textstyle\int_{-\infty}^{\infty} \langle\Phi(0)|\Phi(t)\rangle \; e^{-iEt/\hbar}, \end{aligned} \tag{8}$$

and low resolution versions of equation (7) can be obtained by cutting the associated integration at a finite time [25], or using appropriate filtering [41].

3 Results

In this section we discuss some results obtained from theoretical simulations performed in the spirit of the SEP spectroscopic technique [11]. An initial wave packet is prepared in a location far from the equilibrium position of the molecule, and the corresponding Franck-Condon coefficients calculated. These coefficients are related to the dynamics of the packet [12], thus revealing details of the phase space region in which it started.

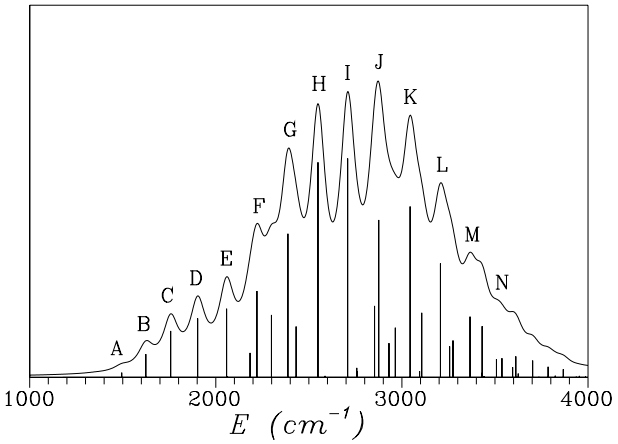

Fig. 2. Stick spectrum and low resolution version of it for a Gaussian wave packet initially centered on the point: $(R,\theta)_0 =$ (3.89 a.u., 87.9°). The low resolution spectrum consists of a series of regularly spaced bands that have been marked A–N.

Let us discuss, for example, the results generated from the minimum uncertainty coherent state

$$|\Phi(0)\rangle = \left(\frac{\alpha_R\alpha_\theta}{\pi\hbar}\right)^{1/2} \exp\left[-\alpha_R^2(R-R_0)^2/2\hbar\right] \times \exp\left[-\alpha_\theta^2(\theta-\theta_0)^2/2\hbar\right] \quad (9)$$

initially located at $(R,\theta)_0 = (3.89\text{ a.u.}, 87.9°)$ and having width parameters $(\alpha_R,\alpha_\theta) = (8.03, 7.51)$ in a.u. With this choice the energy at the center of the packet is 2500 cm^{-1}. To help in the interpretation we have plotted in Figure 1 the contour corresponding to half-height width superimposed to the potential energy surface.

The corresponding stick spectrum, calculated by means of equation (7), is presented in Figure 2. When examined it can be divided into three regions. For energies smaller than $\sim$ 2100 cm^{-1} the spectrum is quite simple. It is formed by a progression of five lines which correspond to the transitions to states increasingly excited in the bending mode [42]; actually $(n_R, n_\theta) = (0, n_b)$ with $n_b = 10{-}18$.

The corresponding wave functions are shown in the first five pannels of Figure 4. They are all very regular [3], appearing the density of probability distributed along the minimum energy path, and being the quantum numbers readily assignable.

Above 2100 cm^{-1} the spectrum becomes less simple to understand: the distribution of energy differences and intensities is more irregular, and no simple progression can be identified. However, the spectrum becomes simpler when low resolution versions of it are considered. For example, we have also plotted in Figure 2, superimposed to the infinite precision stick spectrum, a low resolution version obtained by convolution with Lorentzian functions 100 cm^{-1} wide. In it, a progression of bands regularly spaced is clearly apparent. These bands are formed by clusters of functions, in which the effect of the irregular

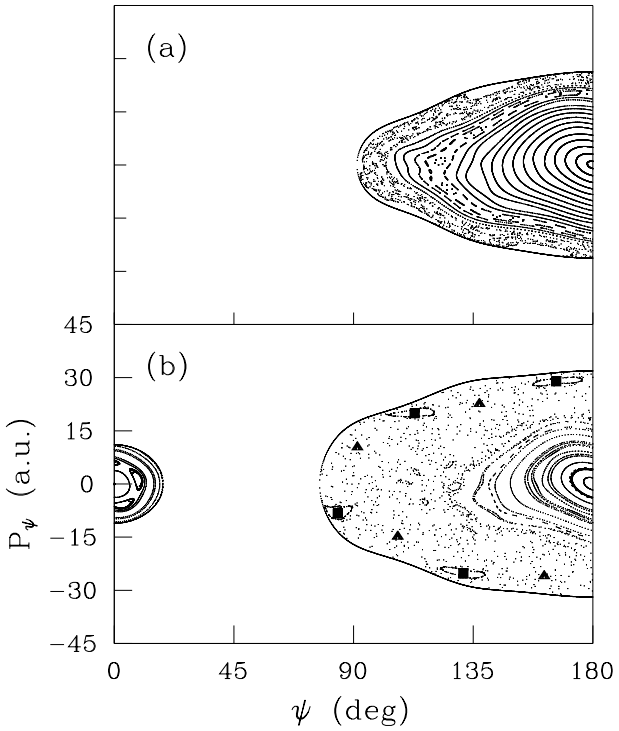

Fig. 3. Classical composite Poincaré surface of section for the LiNC/LiCN system at energies of: (a) 1800 cm^{-1}, and (b) 2500 cm^{-1}. The squares and triangles mark, respectively, the position of the elliptic and hyperbolic fixed points corresponding to the 1:4 periodic orbit of LiNC relevant for the discussion presented in the text.

distribution of intensities and spacings has been averaged out, thus emerging a much more clear pattern. Obviously, these clusters do not contain too many elements, because we are in a regime in which the density of states is low. However, the effect that we are describing is robust, and persists even when the density of states is very high; see for example discussion in reference [25].

In the energy range between $\sim$ 2100−2500 cm^{-1} there appear two bands consisting mainly of just a pair of functions. When examined, these pairs correspond to states $(0,10)$–$(1,6)$ and $(0,11)$–$(1,7)$ respectively, which means that they are "connected" by a 1:4 Fermi resonance. The origin of this interaction has been presented elsewhere [26]. In that paper state correlation diagrams varying $\hbar$ were considered. By doing that, the system can be made artificially more or less chaotic at will. When $\hbar$ is decreased the phase space area needed to "accommodate" a quantum state decreases, and the behaviour of the system becomes more regular. In this way, the mixing exhibited by complex states can be disentangled, just in the opposite way as regular states are mixed in bands F and G of Figure 2 giving scarred structures.

In the third region of the spectrum, corresponding to $E >$ 2500 cm^{-1}, the bands involve a variable number of states; being even some of them, like bands H and I, formed by a single contribution.

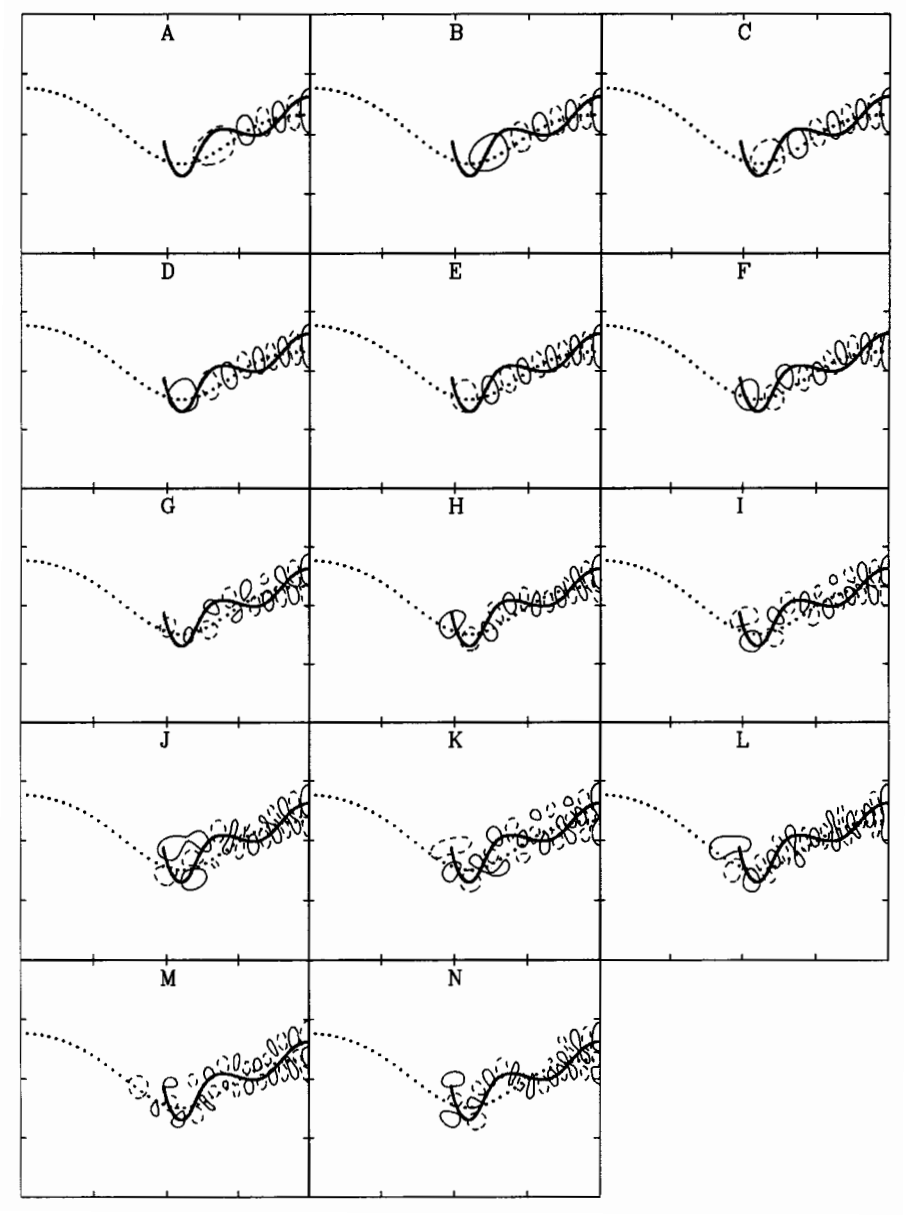

Fig. 4. Wave functions corresponding to the bands A–N appearing in the spectrum of Figure 2. The have been calculated with the projection technique involved in equation (10). The first five functions correspond to the regular states [42] $(n_R, n_\theta) = (0, n_b)$ with $n_b = 10-18$. The axis used are the same as in Figure 1. Negative values of the wave functions are plotted in dashed line.

This behaviour can be compared with the classical counterpart. For that purpose, we show in Figure 3 two composite SOS computed at vibrational energies of 1800 and 2500 cm^{-1}, respectively. At the smaller energy all the dynamics are regular, with SOS formed mainly by closed lines around the fixed point corresponding to the the R motion in the Li–NC isomer $[(\psi, P_\psi) = (180°, 0)]$. Only a narrow band of chaos near the border of the available phase space, caused by the destruction of the outermost invariant tori, is visible.

For $E = 2500$ cm^{-1} the situation is very different. At this energy the LiCN well is barely accessible, showing an conspicuous 1:4 resonance. On the other side, in the LiNC region chaos dominates, and two very distinct regions can be distinguished: the inner one, around the stable Li–NC isomer, which is regular, and the outer one that corresponds to chaotic motion. In this chaotic region we have also marked (with squares and triangles) two POs, stable and unstable respectively, that correspond to a 1:4 resonant chain of islands which is relevant for the discussion below.

This transition from order to chaos reflects at the quantum level. As the energy increases the area of the regular region first increases due to the growth of the available phase space, and then starts to decrease due to the destruction of invariant tori dictated by the KAM theorem. As a result, up to a certain energy value the states have enough "phase space room to accommodate themselves" in the regular region and the increasingly excited bending states look regular, presenting a very clear nodal pattern. For energies above that value the bending states have a significant probability density extending into the chaotic region, and regular states with more excitation in the bending mode (approximately more than 22 quanta)

are no longer found in the quantum calculations. In configuration space this would correspond to states trying to extend beyond the (relatively) sharp curvature in the minimum energy path taking place at $\theta = 99°$ (see Fig. 1). This is in correspondence with the classical bobsled effect [43], by which trajectories coming from the LiNC well and passing beyond that point will inevitably pick up some excitation in the stretching mode in their way back. It is very difficult to make the present argument more quantitative due to the well-known fact that quantum mechanics is somewhat "sluggish" in its response to classical chaos [6,44]. Accordingly, the states which are very extended in θ, present more complicated nodal patterns, some of them being scarred along the stable and unstable trajectories corresponding to the 1:4 PO of Figure 3.

A very useful insight about the nature of the bands observed in the low resolution spectrum of Figure 2 can be gained by using a method developed recently by us [25,34]. Since they correspond to structures which are not well-defined in energy, they must have some sort of resonant-like character. This character can be unveiled by using appropriate calculation technique from resonance theory. For example, one can obtain the corresponding wave functions by Fourier transforming the time-dependent wave packet $|\Phi(t)\rangle$ using a finite time span

$$|\Psi^k\rangle = \frac{1}{2\pi\hbar}\int_{-\tau}^{\tau} dt\ |\Phi(t)\rangle\ e^{-iE_k t/\hbar} = \sum_n |n\rangle\langle n|\Psi(0)\rangle \frac{\sin[(E_k - E_n)\tau/\hbar]}{\pi(E_k - E_n)}, \qquad (10)$$

where E_k represents the energy of the center of the kth band, and τ is of the order of the period of the scarring PO.

In Figure 4 the results corresponding to the different bands appearing in Figure 2 are presented. As can be seen, the wave functions corresponding to bands F–N are more complex than the other five, at least in the sense that their probability densities do not follow the minimum energy path. Actually, if examined closely their maxima appear located, with very good approximation, on the path corresponding to the 1:4 unstable PO of the LiNC/LiCN system mentioned above (triangles in Fig. 3). To guide the eye, this orbit (for an energy of 2500 cm^{-1}) has also been plotted superimposed to the wave functions in the pannels forming Figure 4. This is reasonable since the initial location of the wave packet originating the spectrum of Figure 2 was initiated very close to the turning point of the PO (compare Figs. 1 and 4).

4 Summary and conclusions

In conclusion, in this paper we have presented a study on the relationship existing between dynamics and spectroscopy, by presenting an example corresponding to the molecular vibrations of the LiNC/LiCN molecular system. This system has been extensively studied in the literature in connection with quantum chaos. It can be described quite realistically with a simple model, for which the motion in the angular bending coordinate is very floppy, so that chaos sets in at low excitation energies. We have illustrated how the short term dynamics of a wave packet reflects in the low resolution features of molecular spectra such as SEP. For a wave packet initially located in a very chaotic region, we have shown how a particular PO influences all the dynamics, and the low resolution bands of the resulting spectrum correspond to wave functions structures which are profoundly influenced by this PO. These bands can be formed by a single, and then already scarred, state or more, depending on the energy range we are considering. Obviously, the very low energy end of the spectrum, for which the PO we are referring to has not even appeared, is totally regular.

We think that the theoretical tools we have discussed in this paper, which continue the path initiated by others [12,23,24,33], constitute a great help in the understanding of the structure observed in the spectra of classically chaotic systems.

This work has been supported in part by DGES (Spain) under Projects No. PB95-425 and PB96-76.

References

1. R. Schienke, *Photodissociation Dynamics* (Cambridge University Press, Cambridge, 1992).
2. G. Herzberg, *Molecular Spectra and Molecular Structure II. Infrared and Raman Spectra of Polyatomic Molecules* (Van Nostrand, Princeton, 1964).
3. R.M. Stratt, N.C. Handy, W.H. Miller, J. Chem. Phys. **71**, 3311 (1979).
4. V.B. Chirikov, Phys. Rep. **52**, 263 (1979).
5. C. Jaffé, P. Brumer, J. Chem. Phys. **73**, 5646 (1980); E.L. Sibert III, W.P. Reinhardt, J.T. Hynes, J. Chem. Phys. **77**, 3583 (1982).
6. N. De Leon, M.J. Davis, E.J. Heller, J. Chem. Phys. **80**, 794 (1984).
7. V.I. Arnold, *Mathematical Methods of Classical Mechanics* (Springer-Verlag, New York, 1978).
8. L.E. Reichl, *The Transition to Chaos in Conservative Classical Systems: Quantum Manifestations* (Springer-Verlag, New York, 1992).
9. T. Uzer, Phys. Rep. **199**, 75 (1991); S.A. Schofield, P.G. Wolynes, R.E. Wyatt, Phys. Rev. Lett. **74**, 3720 (1995).
10. *Laser Spectroscopy of Highly Vibrationally Excited Molecules*, edited by V.S. Letokhov (Adams Hilger, New York, 1989).
11. *Molecular Dynamics and Spectroscopy by SEP*, edited by H.L. Dai, R.W. Field (World Scientific, Singapore, 1995).
12. E.J. Heller, J. Chem. Phys. **62**, 1544 (1975); *Chaos and Quantum Physics*, edited by M. Giannoni, A. Voros, J. Zinn-Justin (Elsevier, Amsterdam, 1991).
13. C. Leforestier, R. Bisseling, C. Cerjan, M.D. Feit, R. Friesner, A. Guldberg, A. Hammerich, G. Jolicard, W. Karrlein, H.D. Meyer, N. Lipkin, O. Roncero, R. Kossloff, J. Comput. Phys. **94**, 59 (1991).
14. Z. Bačić, J. Light, Ann. Rev. Phys. Chem. **40**, 469 (1989).

15. D.T. Colbert, E.L. Sibert III, J. Chem. Phys. **91**, 350 (1989).
16. H. Goldstein, *Classical Mechanics* (Addisom-Wesley, Reading, 1980).
17. M.C. Gutzwiller, *Chaos in Classical and Quantum Mechanics* (Springer, New York, 1990); K. Nakamura, *Quantum Chaos. A New Paradigm of Nonlinear Dynamics* (Cambridge University Press, Cambridge, 1993).
18. E.N. Lorenz, *The Essence of Chaos* (University College London Press, London, 1995).
19. E.J. Heller, Phys. Rev. Lett. **53**, 1515 (1984).
20. S.W. McDonald, A.N. Kaufmann, Phys. Rev. Lett. **42**, 1189 (1979); Phys. Rev. A **37**, 3067 (1988).
21. M.V. Berry, J. Phys. A **10**, 2083 (1977); A. Voros, in *Stochastic Behaviour in Classical and Quantum Hamiltonian Systems*, edited by G. Casati, J. Ford (Springer, Berlin, 1979).
22. A.I. Shnirelman, Ups. Mat. Nauk. **29**, 181 (1974).
23. M.C. Gutzwiller, J. Math. Phys. **12**, 343 (1971); Phys. Rev. Lett. **45**, 150 (1980).
24. E.B. Bogomolny, Physica D **31**, 169 (1988).
25. G.G. de Polavieja, F. Borondo, R.M. Benito, Phys. Rev. Lett. **73**, 1613 (1994).
26. F.J. Arranz, F. Borondo, R.M. Benito, Phys. Rev. Lett. **80**, 944 (1998).
27. P. Leboeuf, A. Voros, J. Phys. A **23**, 1765 (1990); M.B. Cibils, Y. Cuche, P. Leboeuf, W.F. Wreszinski, Phys. Rev. A **46**, 4560 (1992).
28. K. Husimi, Proc. Phys. Soc. Jpn **22**, 264 (1940).
29. F.J. Arranz, F. Borondo, R.M. Benito, Phys. Rev. E **54**, 2458 (1996); J. Mol. Struct. (THEOCHEM) **426**, 87 (1998).
30. G. Tanner, P. Scherer, E.B. Bogomolny, B. Eckhardt, D. Wintgen, Phys. Rev. Lett. **67**, 2410 (1991).
31. M.A. Iken, F. Borondo, R.M. Benito, T. Uzer, Phys. Rev. A **49**, 2734 (1994).
32. Remember the Fourier transform relation existing between spectrum and correlation function (see Eq. (8) in Sect. 2 below.)
33. J.M. Gomez-Llorente, E. Pollak, Ann. Rev. Phys. Chem. **43**, 91 (1992); H.S. Taylor, Acc. Chem. Res. **22**, 263 (1989).
34. J.M. Gomez-Llorente, N. Berenger, F. Borondo, R.M. Benito, Chem. Phys. Lett. **192**, 430 (1992).
35. F. Borondo, R.M. Benito, *Frontiers of Chemical Dynamics*, NATO ASI Ser. C, edited by E. Yurtsever (Kluwer, Dordrecht, 1995) and references therein.
36. R. Essers, J. Tennyson, P.E.S. Wormer, Chem. Phys. Lett. **89**, 223 (1982).
37. J. Makarewitz, T. Ha, J. Molec. Struct. (THEOCHEM) **315**, 149 (1994); Chem. Phys. Lett. **232**, 497 (1995).
38. F. Borondo, A.A. Zembekov, R.M. Benito Chem. Phys. Lett. **246**, 421 (1995); J. Chem. Phys. **105**, 5068 (1996); *ibid.* **107**, 7934 (1997).
39. R.M. Benito, F. Borondo, J.-H. Kim, B.G. Sumpter, G.S. Ezra, Chem. Phys. Lett. **161**, 60 (1989).
40. Z. Bačić, J. Light, J. Chem. Phys. **85**, 4594 (1986).
41. W.H. Press, B.P. Flannery, S.A. Teukolsky, W.T. Vettering, *Numerical Recipes: The Art of Scientific Computing* (Cambridge University Press, Cambridge, 1986).
42. Although the range spanned by the angular variable θ goes from 0 to π we use for the regular states the notation corresponding to a harmonic description, in which the quantum bending number corresponds to double the number of nodes in θ. The quantum number can only be even due to the fact that we are only considering states with total angular momentum equal to zero ($J = 0$). See discussion in I.N. Levine, *Molecular Spectroscopy* (Wiley, New York, 1975), p. 271.
43. W.H. Miller, J. Chem. Phys. **72**, 99 (1980).
44. W.P. Reinhardt, C. Jaffé, *Quantum Mechanics in Mathematics, Chemistry and Physics*, edited by K.E. Gustavson, W.P. Reinhardt (Plenum, New York, 1981).